

## **General Disclaimer**

### **One or more of the Following Statements may affect this Document**

- This document has been reproduced from the best copy furnished by the organizational source. It is being released in the interest of making available as much information as possible.
- This document may contain data, which exceeds the sheet parameters. It was furnished in this condition by the organizational source and is the best copy available.
- This document may contain tone-on-tone or color graphs, charts and/or pictures, which have been reproduced in black and white.
- This document is paginated as submitted by the original source.
- Portions of this document are not fully legible due to the historical nature of some of the material. However, it is the best reproduction available from the original submission.

(NASA-CR-174410) MATERIAL GROWTH AND  
CHARACTERIZATION FOR SOLID STATE DEVICES  
Annual Report, 1 Dec. 1983 - 30 Nov. 1984  
(North Carolina Agricultural and Technical)  
22 p HC A02/MF A01

N85-19847

Unclas  
14260

CSCI 20L G3/76

NORTH CAROLINA A&T STATE UNIVERSITY

Department of Electrical Engineering  
Greensboro, North Carolina 27411

ANNUAL REPORT

on

MATERIAL GROWTH AND CHARACTERIZATION FOR  
SOLID STATE DEVICES

NASA Grant - HSG 1390

PERIOD: December 1, 1983 to November 30, 1984

CONTRIBUTORS

E. K. Stefanakos  
W. J. Collis  
A. Abul-Fadl  
S. Iyer



## TABLE OF CONTENTS

	<u>Page</u>
SUMMARY. . . . .	ii
GROWTH OF InGaAs. . . . .	1
SIMS MEASUREMENTS. . . . .	4
SELECTIVE GROWTH OF InGaAs ON InP . . . . .	8
GROWTH AND CHARACTERIZATION OF InGaAsP AND InP. . . . .	11
INSULATOR STUDIES FOR MISFET DEVICES. . . . .	16
REFERENCES. . . . .	19

# MATERIAL GROWTH AND CHARACTERIZATION FOR SOLID STATE DEVICES

## SUMMARY

The program objectives for this period have been to investigate:

- (a) dopants for InP and InGaAs incorporated in epilayers during CCLPE growth;
- (b) insulator deposition on InGaAs; and (c) diffused junction and selective area growth for the fabrication of electronic devices.

Manganese (Mn) was used as the dopant for p-type InGaAs layers grown on semi-insulating (Fe-doped) and n-type (Sn-doped) InP substrates. Optical, electrical (Hall) and SIMS measurements were performed in order to characterize the layers. Mn-diffusion into the substrate (during the growth of InGaAs) was observed only when Fe-doped substrates were used.

Quaternary layers of two compositions corresponding to wavelengths (energy gaps) of  $\approx 1.52\mu\text{m}$  were successfully grown at a constant temperature of  $640^\circ\text{C}$  by the CCLPE technique. Growth of InP was also carried out in the temperature range of  $640\text{--}655^\circ\text{C}$ . A study was performed to determine the effect of pulses on the growth velocity of InP. The results indicated no significant change as long as the average applied current was kept constant.

A system for depositing films of  $\text{Al}_2\text{O}_3$  by the pyrolysis of aluminum isopropoxide was designed and built during this period. Deposited layers on Si were characterized with an ellipsometer and exhibited indices of refraction between 1.582 and 1.622 for films on the order of  $3000\text{ \AA}$  thick.

Undoped and p-type (Mn-doped) InGaAs epitaxial layers were also grown on Fe-doped InP substrates through windows in sputtered  $\text{SiO}_2$  ( $3200\text{ \AA}$  thick) layers. The mask geometries were Hall patterns defined by standard photolithographic techniques using AZ-photoresist.

## Growth of InGaAs

Undoped and p-type manganese (Mn) doped layers of InGaAs, lattice matched to (100) Fe-doped and n-type tin (Sn) doped InP substrates, were grown by CCLPE. The layers were grown at a constant furnace temperature of 640°C and a current density of 5A/cm<sup>2</sup> for 30 minutes. The undoped layers were in the high 10<sup>15</sup>cm<sup>-3</sup> to low 10<sup>16</sup>cm<sup>-3</sup> carrier concentration range.

The p-type layers were grown using Mn as an acceptor. The amount of Mn used to dope the InGaAs melts was based on a Mn distribution coefficient of  $k_{Mn} \approx 0.1 - 0.3$  [1] and on the desired level of acceptors. A 10<sup>17</sup>cm<sup>-3</sup> acceptor level and an indium melt weight of  $\approx 4.3$  grams required about 60 micrograms of Mn. The manganese was selected because of its low vapor pressure as compared to Zn, Mg or Cd and being not as toxic as beryllium.

Table I gives a summary of Hall measurements performed on undoped and Mn-doped layers. The carrier concentration and mobility of p-type layers were in the range reported by Chad et. al [2] in close agreement with a manganese distribution coefficient of  $k_{Mn} \approx 0.3$ .

Cleaved sections of Mn-doped layers showed, in addition to the grown layer a diffusion tail. Figure 1a shows a 20.35μm diffused layer which resulted after a 3.7μm Mn-doped layer was grown using 5A/cm<sup>2</sup> and 30 minutes. Figure 1b shows that the diffused layer is limited to the region of contact between the melt and substrate. This clearly indicates that diffusion of Mn takes place during growth. Mn-doped layers grown on n-type substrates did not produce diffused layers. This is because the diffusion tail is overcompensated by the more highly n-doped substrate. To investigate the property of this diffused layer, Hall measurements were performed on the grown layer (including the diffused layer) using only the thickness of the grown layer in the Hall calculations. Subsequently, the grown layer was

TABLE I. GROWTH OF InGaAs BY CCLPE

SAMPLE #	TYPE	GROWTH TEMP. (°C)	STEP COOLING $\Delta T$ (0°C)	CURRENT DENSITY (A/m <sup>2</sup> )	GROWTH TIME (mins.)	EPI-LAYER THICKNESS ( $\mu$ m)	DIFFUSED LAYER THICKNESS ( $\mu$ m)	MOBILITY AT ROOM TEMP. (cm <sup>2</sup> /VS)	CARRIER CONC. $\times 10^{16}$ (cm <sup>-3</sup> ) (300k)
IIA-I	n(U)	640	0	2.5	60	4.38	0	12437.30	4.17
IIB-1	n(U)	640	0	10	15	2.55	0	8283.72	6.42
IIB-2	n(U)	640	0	5	15	1.5	0	6703.52	3.49
IIB-4	n(U)	640	0	5	15	3.7	0	9669.31	0.87
	n(U)							10,000.	2.0 <sup>1</sup>
	n(U)							9,000.	0.006 <sup>2</sup>
	n(U)							12,800.	0.52 <sup>3</sup>
	n(U)							11,200	0.05 <sup>4</sup>
	n(U)							13,800	0.15 <sup>5</sup>
IIA-4	p(Mn)	640	5	0	30	3.70	20.35	135.99	52.57
IIA-6	p(Mn)	640	5	0	15	2.92	14.80	116.22	60.40
IIA-7	p(Mn)	640	0	10	15	2.20	14.80	136.93	47.68
IIB-5	p(Mn)	640	2.5	5	30	11.0	9.25	175.43	17.55
IIB-7	p(Mn)	640	2.5	5	30	9.25	9.25	---	---
	p(Mn)							183.0	15.06 <sup>6</sup>

U - Undoped

Mn - Manganese

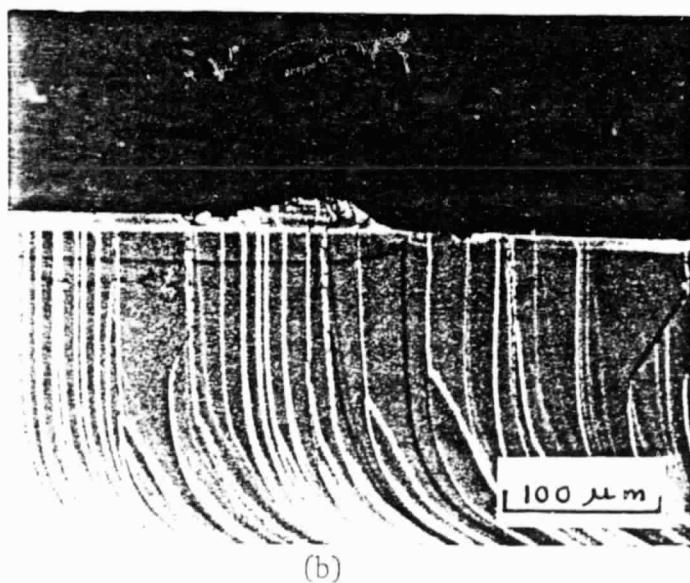
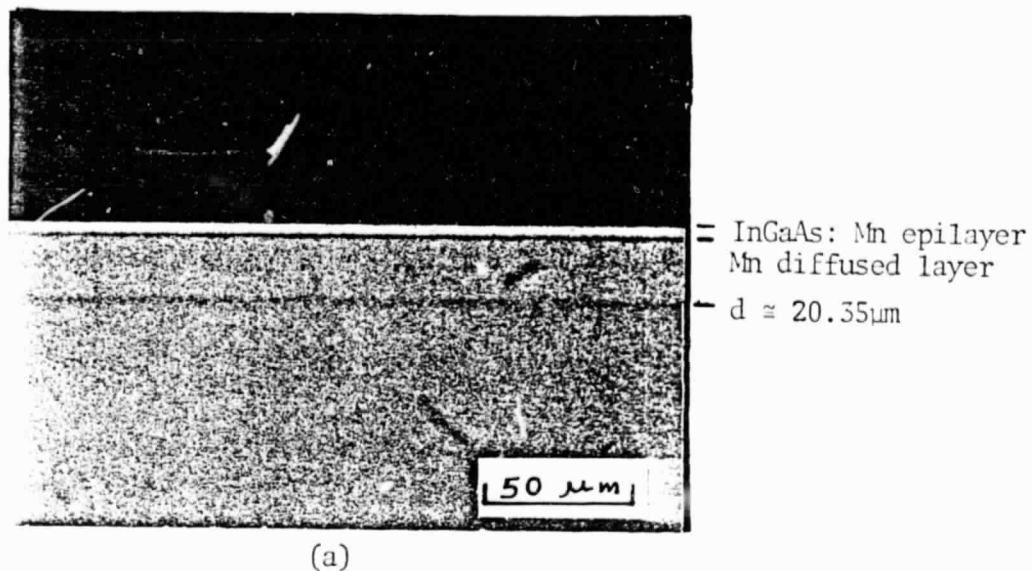


Figure 1 Photomicrographs of stained cleavages of InGaAs: Mn/InP (Fe):  
 (a) The deep diffusion of Mn into the semi-insulating substrate took place during the LPE/CCLPE growth.  
 (b) Diffusion of Mn is limited to melt-substrate contact area.

ORIGINAL PAGE  
 BLACK AND WHITE PHOTOGRAPH

selectively etched using  $1\text{H}_2\text{O}_2:1\text{H}_2\text{O}:5\text{H}_2\text{SO}_4$  at room temperature, except for the four contact areas (the indium dots and the layer under the dots). Hall measurements were then performed on the diffused layer and the results indicated an average carrier concentration in the  $2\text{--}3 \times 10^{15}\text{ cm}^{-3}$  range, about two orders of magnitude below the carrier concentration in the epi-layer. The thickness of the diffused layer varied with the growth conditions. As the concentration of Mn in the melt increased from  $2.8 \times 10^{-5}\text{ A/O}$ , ( $p \approx 1.7 \times 10^{17}$ ) to  $7.78 \times 10^{-5}\text{ A/O}$  ( $p \approx 6.4 \times 10^{17}$ ) the thickness of the diffused layer increased from 9.25 to  $20.35\mu\text{m}$  (the growth time and melt saturation time were kept constant). Shorter growth times resulted in reduced thickness of the diffused layer. Another factor, the melt saturation time did not play an important role in determining the depth of diffusion. For most layers, the growth melt and substrate were baked overnight for about 17 hours (the substrate was kept under an In-Sn-P basket for protection from thermal deterioration). Reducing the melt bake time to less than 2 hours showed no reduction in thickness of the diffused layer.

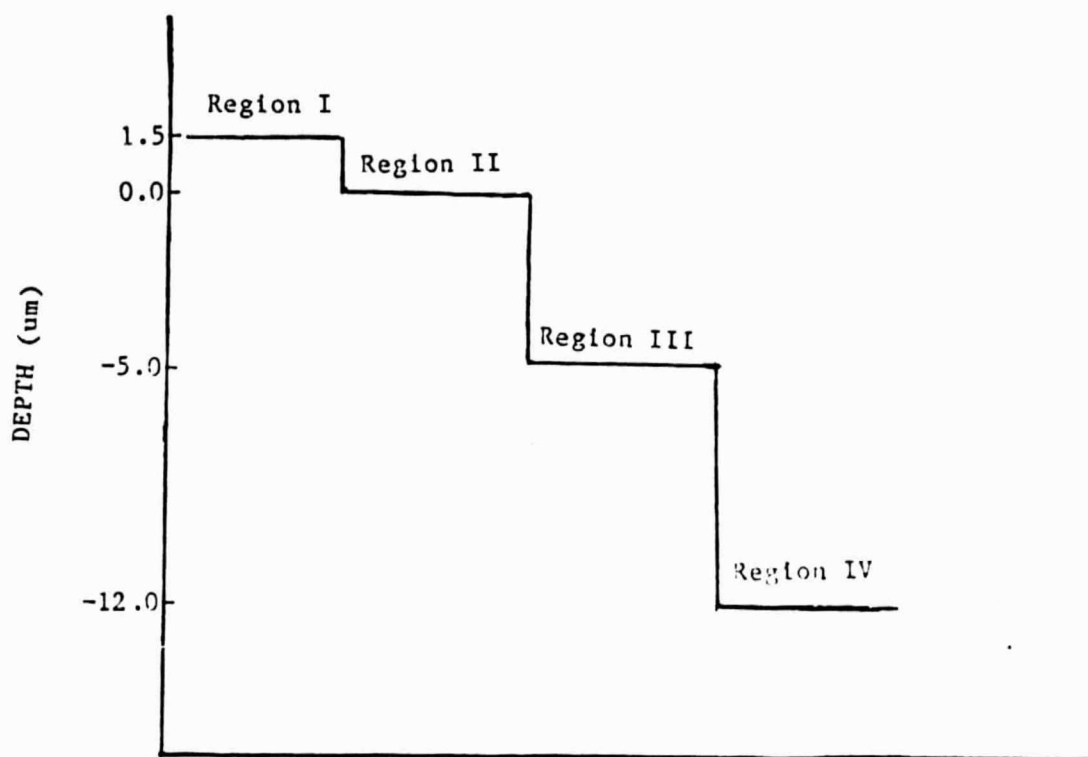
### SIMS Measurements

SIMS measurements were carried out to determine the doping profile of InGaAs layers grown on semi-insulating InP substrates after step etching various regions using nitric acid and a bromine-methanol (2%) solution. Figure 2 shows Tencor step-profiler measurements made on the sample throughout the etching process. Each region approximately represents one quarter of the same surface.

Interpretation of SIMS spectra is complicated by the wide range of secondary ion yields encountered for different species on a surface. The doping profile shown in Figure 3 was obtained by comparing

layer	substrate
Region I	Region II
-5um	-12um
RegionIII	Region IV

(a)



(b)

Figure 2. (a) Definition of the four regions: region I is the epilayer and the substrate; region II is the substrate after etching the epilayer; region III is the substrate after etching the epilayer and 5um of the substrate; and region IV is the substrate after etching the epilayer and 12um of the substrate. (b) corresponding depth-profile.

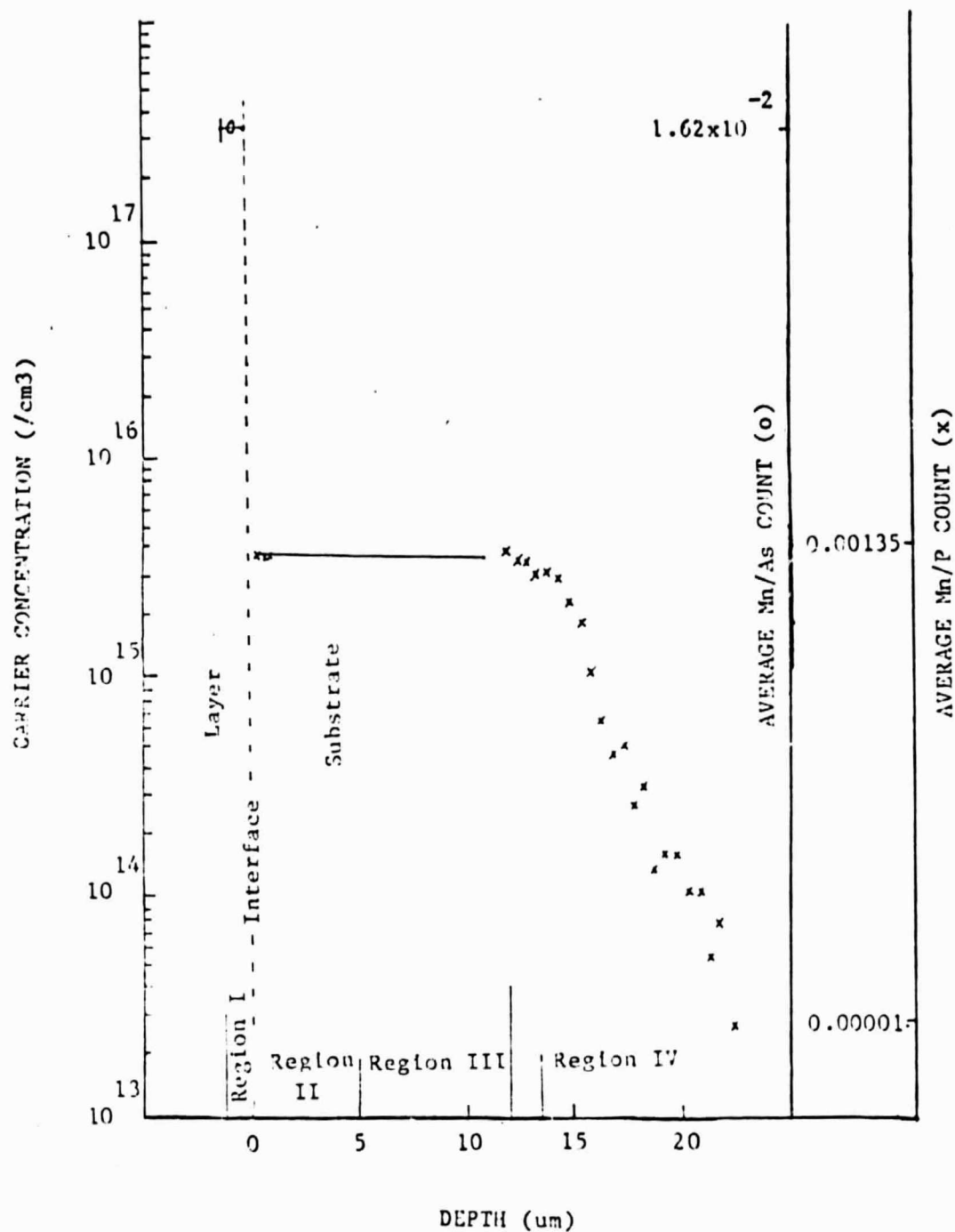


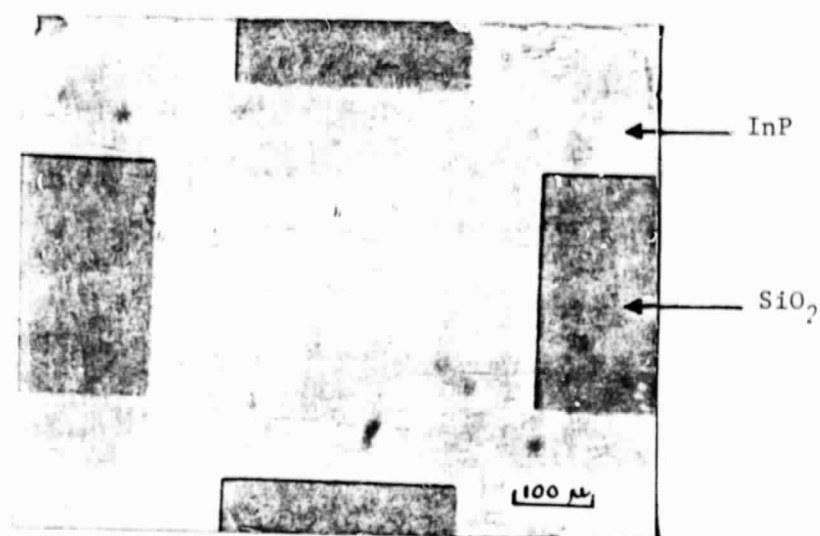
Figure 3. Semi-quantitative doping profile of Mn in InGaAs-InP(Fe), as predicted from SIMS data, and Hall measurements on the grown layer and the diffused layer. o, x indicate average Mn/As and Mn/P count in the grown layer and in the substrate, respectively. The solid line indicates the average carrier concentration as determined from Hall measurements.

the ratios of Mn/As and Mn/P to reference ratios ( $\text{Mn/As} = 1.62 \times 10^{-2}$  and  $\text{Mn/P} = 1.35 \times 10^{-3}$ ) obtained from Hall measurements on the epilayer. Figure 3 shows that at the epilayer-substrate interface the carrier concentration decreases by about two orders of magnitude and remains constant up to a depth of  $12\mu\text{m}$  in the substrate and up to the interface between the diffused layer and the semi-insulating substrate. Similar results have been reported by SpringThorpe et. al [7] in the case of Zn diffusion in InGaAs.

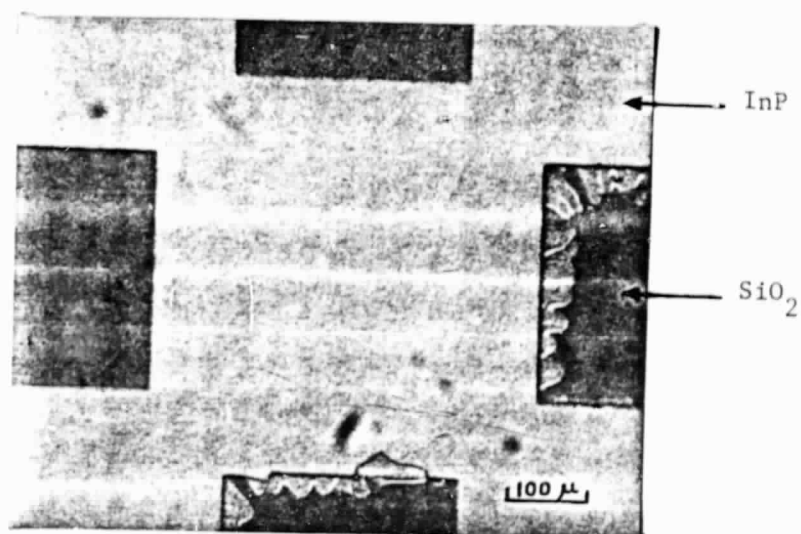
### Selective Growth of InGaAs on InP

Undoped and p-type Mn-doped InGaAs epitaxial layers were grown on (100) Fe-doped InP substrates through windows in an  $\text{SiO}_2$  mask ( $3200\text{\AA}$  thick). The mask geometry (Hall pattern) was defined by the standard photolithography technique using AZ - photoresist and sputtered  $\text{SiO}_2$ . The substrates were chemically cleaned and etched in a 0.1% by volume  $\text{Br}_2\text{CH}_3\text{OH}$  etch or in a Caro-etch ( $5\text{H}_2\text{SO}_4:1\text{H}_2\text{O}_2:1\text{H}_2\text{O}$ ) at room temperature, for about 10 seconds. Both solutions gave rise to slight undercutting in some regions after etching time of 20 seconds or more. Figures 4a and 4b show samples etched with Caro-etch at room temperature for 10 sec and 20 sec. respectively. Heat treatment at the growth temperature of  $640^\circ\text{C}$ , of the masked substrate without phosphorous overpressure, resulted in thermal degradation of the regions not covered with  $\text{SiO}_2$ . No noticeable degradation was observed under the  $\text{SiO}_2$  masked regions. To protect the unmasked regions, phosphorous over-pressure from an In-Sn-P solution was used during LPE growth.

The LPE growth was carried out using either step cooling of  $3^\circ\text{C}$  or isothermally with a current density of  $5\text{A}/\text{cm}^2$  and 30 minutes. Figure 5 shows an epitaxial film of Mn-doped InGaAs growth through the  $\text{SiO}_2$  mask. Except for a slight edge growth around the growth region, the growth is very uniform. A diffused layer can also be seen. The diffused layer is because of Mn diffusion during the growth of the film. Again, as described earlier, the diffusion is limited to the growth area, with some lateral diffusion, and the  $\text{SiO}_2$  film seems to work very well as a mask for growth as well as for the diffusing impurities.



(a)



(b)

Figure 4. Photomicrographs showing InP samples masked with SiO<sub>2</sub>. (a) Sample etched with Caro-etch for 10 seconds at room temperature. (b) Sample etched with Caro-etch for 20 seconds at room temperature suffered slight undercutting near some SiO<sub>2</sub> edges.

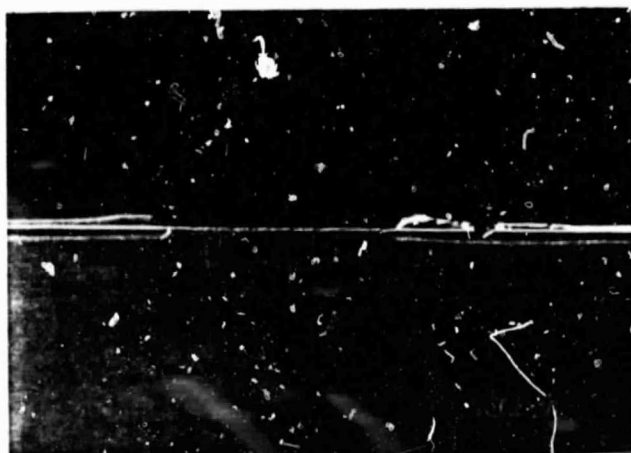


Figure 5. Selective growth of Mn-doped InGaAs layer on an InP substrate by combined LPE (step cooling of 3°C) and CCLPE (5A/cm<sup>2</sup>) for 30 minutes. The observed tapering near the edges of the SiO<sub>2</sub> mask is attributed primarily to higher current densities.

ORIGINAL PAGE  
BLACK AND WHITE PHOTOGRAPH

## Growth and Characterization of InGaAsP and InP

During this period the growth rate and kinetics of growth of  $\text{In}_{1-x}\text{Ga}_x\text{As}_y\text{P}_{1-y}$  quaternary and InP layers lattice matched to InP by the CCLPE technique have been studied. The aim of the study was to grow these layers of low impurity levels with uniform thickness and smooth morphology for the purpose of utilizing them in electronic and optoelectronic devices e.g., photodiodes, LED's and MISFET's.

### InGaAsP

Quaternary layers of two compositions of energy gaps corresponding to wavelengths of  $\approx 1.52\mu\text{m}$  and  $\approx 1.31\mu\text{m}$  have been successfully grown at a constant furnace temperature of  $640^\circ\text{C}$  by the CCLPE technique. The growth was carried out in a conventional horizontal slider boat system. The growth procedure has been described in detail in Ref. 8. A good lattice match with  $\frac{\Delta a}{a} \approx 0.04\%$  has been achieved in these layers. On using the same melt for consecutive growth runs, lattice mismatch increases with corresponding shifts in photoluminescence peak wavelength and changes in surface morphology of the epilayers. A maximum shift of  $\approx 600\text{\AA}$  was observed in  $\text{In}_{.60}\text{Ga}_{.40}\text{As}_{.85}\text{P}_{.15}$  layers, while the shift in  $\text{In}_{.73}\text{Ga}_{.27}\text{As}_{.60}\text{P}_{.40}$  samples was significantly less ( $\approx 160\text{\AA}$ ) as illustrated in Tables II and III, respectively. The surface morphology of the surface changed from terraced to cross-hatched pattern. The maximum thickness of the layers that could be grown was limited to  $\approx 5\mu\text{m}$  for  $\text{In}_{.60}\text{Ga}_{.40}\text{As}_{.85}\text{P}_{.15}$  samples and  $\approx 3\mu\text{m}$  for  $\text{In}_{.73}\text{Ga}_{.27}\text{As}_{.60}\text{P}_{.40}$  samples. This may be attributed to the increase in lattice mismatch resulting in degradation of the layer surface.

Growth velocity of the quaternary layer exhibits a linear dependence with current density; current density varying up to  $20\text{A}/\text{cm}^2$ . Further, the growth velocity is found to be a function of the epilayer composition varying from  $0.62\mu\text{m}/\text{min}$  for  $\text{In}_{.53}\text{Ga}_{.47}\text{As}$  to  $0.03\mu\text{m}/\text{min}$  for  $\text{In}_{.73}\text{Ga}_{.27}\text{As}_{.60}\text{P}_{.40}$  samples, at a current density of  $10\text{A}/\text{cm}^2$ . This result has been satisfactorily accounted by the growth kinetics model, assuming the electromigration of the solute to be the dominant mechanism.

### InP

Growth of InP layers on (100)-oriented InP substrates was carried out in the temperature range of  $640\text{--}655^\circ\text{C}$ . The growth velocity was typically  $\approx 2.3\mu\text{m}/\text{hr}$  at a current density of  $10\text{A}/\text{cm}^2$ . On increasing the growth temperature to  $680^\circ\text{C}$ , the growth velocity increased to  $5.5\mu\text{m}/\text{hr}$ . The growth velocity of these layers also varies linearly with current density as indicated in Fig. 6. A study was also carried to determine the effect of pulses on the growth velocity of InP, as it has been reported [9] that the growth velocity of GaAs layers could be enhanced by decreasing the pulse duration over the normal growth velocity obtained by passing DC current of an equivalent density. However, no such increase in the growth velocity of InP was observed on varying the pulse duration from  $50\mu\text{sec}$  to  $10\text{msec}$  (peak current density was maintained within  $35\text{--}50\text{A}/\text{cm}^2$ ).

The carrier concentrations of these layers were typically  $\approx 10^{17}/\text{cm}^3$  with room temperature mobilities of  $2000\text{cm}^2/\text{V}\text{-sec}$ . The high carrier concentration in these samples was traced to a small leak through the two current carrying electrodes of the system.

Work is being continued to optimize the duration of baking and baking temperature of the melt to obtain lower carrier concentrations with high mobility. Further, these layers will be doped with p-type impurity and the effect of pulses would be studied.

TABLE II. PHOTOLUMINESCENCE MEASUREMENTS FOR  $\text{In}_{0.60}\text{Ga}_{0.40}\text{As}_{0.85}\text{P}_{0.15}$  (average composition)

SAMPLE NUMBER	PEAK WAVELENGTH ( $\mu\text{m}$ )	ENERGY GAP (eV)	SOLIDUS COMPOSITION
H' 3	1.56	0.79	$\text{In}_{0.59}\text{Ga}_{0.41}\text{As}_{0.86}\text{P}_{0.14}$
H' 4	1.54	0.80	$\text{In}_{0.60}\text{Ga}_{0.40}\text{As}_{0.84}\text{P}_{0.16}$
H' 5	1.52	0.81	$\text{In}_{0.61}\text{Ga}_{0.39}\text{As}_{0.82}\text{P}_{0.18}$
H' 6	1.49	0.83	$\text{In}_{0.62}\text{Ga}_{0.38}\text{As}_{0.80}\text{P}_{0.20}$

TABLE III. PHOTOLUMINESCENCE MEASUREMENTS FOR  $\text{In}_{0.73}\text{Ga}_{0.27}\text{As}_{0.60}\text{P}_{0.40}$  (average composition)

SAMPLE NUMBER	PEAK WAVELENGTH ( $\mu\text{m}$ )	ENERGY GAP (eV)	SOLIDUS COMPOSITION
T' 5	1.326	0.93	$\text{In}_{0.70}\text{Ga}_{0.30}\text{As}_{0.62}\text{P}_{0.38}$
T' 6	1.324	0.93	$\text{In}_{0.71}\text{Ga}_{0.29}\text{As}_{0.61}\text{P}_{0.39}$
T' 7	1.318	0.94	$\text{In}_{0.72}\text{Ga}_{0.28}\text{As}_{0.60}\text{P}_{0.40}$
T' 9	1.310	0.94	$\text{In}_{0.72}\text{Ga}_{0.28}\text{As}_{0.59}\text{P}_{0.41}$
U' 1	1.310	0.94	$\text{In}_{0.72}\text{Ga}_{0.28}\text{As}_{0.59}\text{P}_{0.41}$

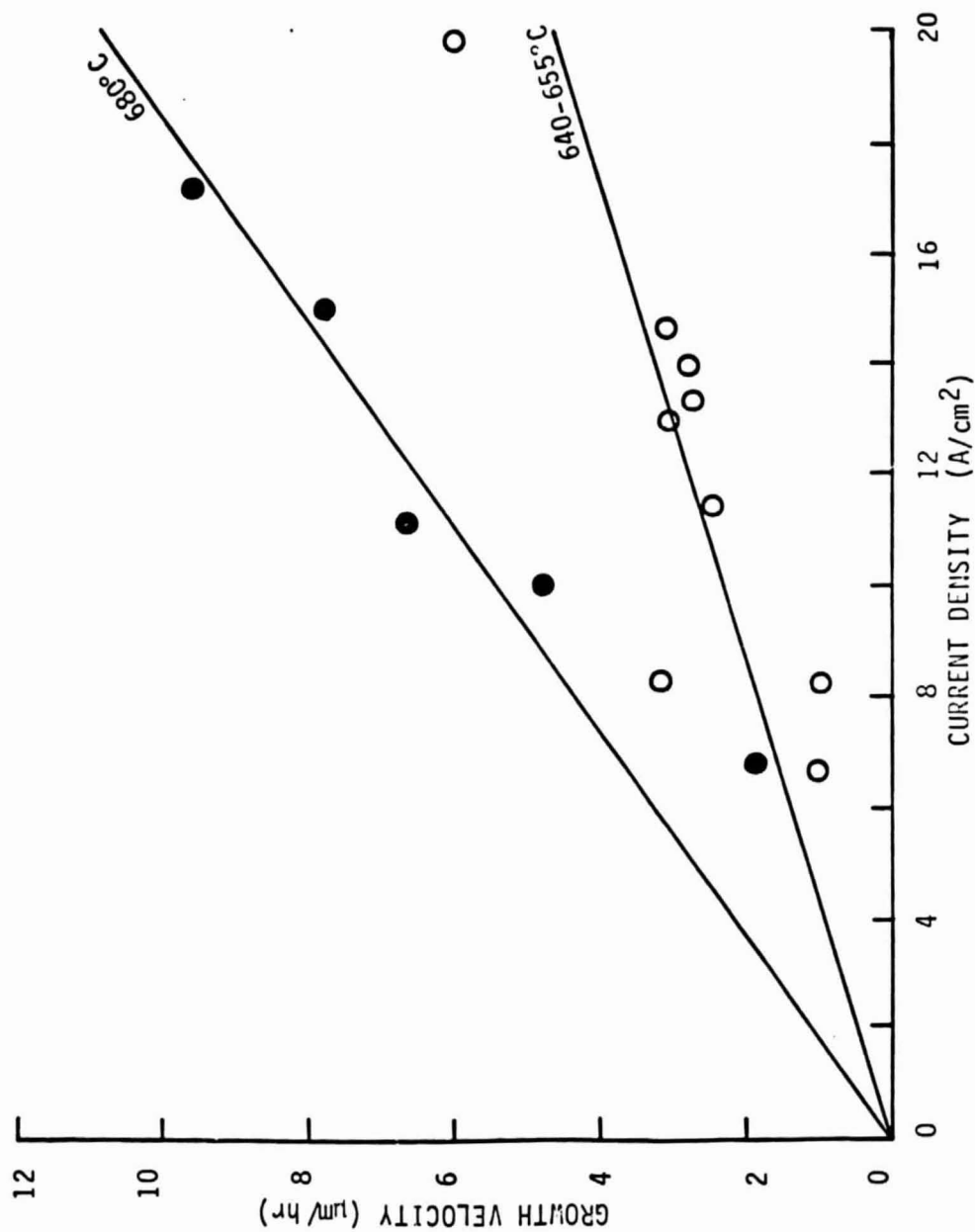


Figure 6. Growth velocity vs. current density of InGaAsP grown by CCLPE on semi-insulating InP substrates at 650°C and 680°C.

### Insulator Studies for MISFET Devices

A system for depositing films of  $\text{Al}_2\text{O}_3$  by the pyrolysis of aluminum isopropoxide is operational. The substrates are placed on a graphite susceptor in a horizontal quartz-reaction tube. This susceptor is heated to 300-400°C by a quartz-halogen lamp array. Argon has been used as the main gas flow, as well as the carrier gas which passes through the heater aluminum isopropoxide reservoir. The growth rate is about 100 Å/min. Hydrogen has also been used as the carrier gas, but no significant difference was observed in the physical quality of the films. One difficulty is the presence of the pinholes in some of the grown layers. These create defects in the metal-insulator-semiconductor capacitors which are formed in order to evaluate the oxide properties. Obviously, growth conditions should be selected which result in a small pinhole density, but the cause is not immediately obvious. There is considerable deposition upon the reactor tube and downstream from the susceptor. Small particles of oxide from the surface of the susceptor or the reaction tube may lead to the pinhole problem. This defect problem can be temporarily solved by evaporating sapphire over the CVD-deposited  $\text{Al}_2\text{O}_3$  before depositing the gate metal.

Over a one centimeter square substrate there is observed a variation in thickness as evidenced by a variation in interference color. A better thickness uniformity is achieved by placing the lamp array above the susceptor. In attempting to mask and etch steps in the  $\text{Al}_2\text{O}_3$  films in order to measure the thickness with a surface profiler, it was discovered that individual films exhibited considerably different etching characteristics. Some layers were characterized with an ellipsometer at the Microelectronics Center of North Carolina. The index of refraction varied from 1.582 to 1.622 for films on order of 3000 Å thick.

Most layers were deposited on Si substrates during the deposition evaluation. A typical capacitance-voltage (C-V) characteristic, measured at 1 MHz with an Al gate is shown in Figure 7. The C-V hysteresis loop width is about 1 volt for a gate voltage rate of 0.4V/sec. Some  $\text{Al}_2\text{O}_3$  films were deposited on nGaAs substrates. The capacitance of the fabricated MIS diodes was essentially constant over a  $\pm 10$  volt gate bias range at 1MHz. Thus, there is a considerable contrast between the Si and GaAs- $\text{Al}_2\text{O}_3$  interface properties.

Efforts are now directed at obtaining the necessary pGaInAs layers for investigating the properties of the deposited  $\text{Al}_2\text{O}_3$ . A system to produce  $\text{H}_2 + \text{HCl}$  by reducing  $\text{MoCl}_5$  is being constructed. This will be used to remove any residual III-V oxides on the substrate surface prior to  $\text{Al}_2\text{O}_3$  deposition.

A scanning electron microscope (ISI SS-40) has been purchased by the School of Engineering and is presently being installed. This should aid in studying the p-n junction structures formed by epitaxial growth and diffusion.

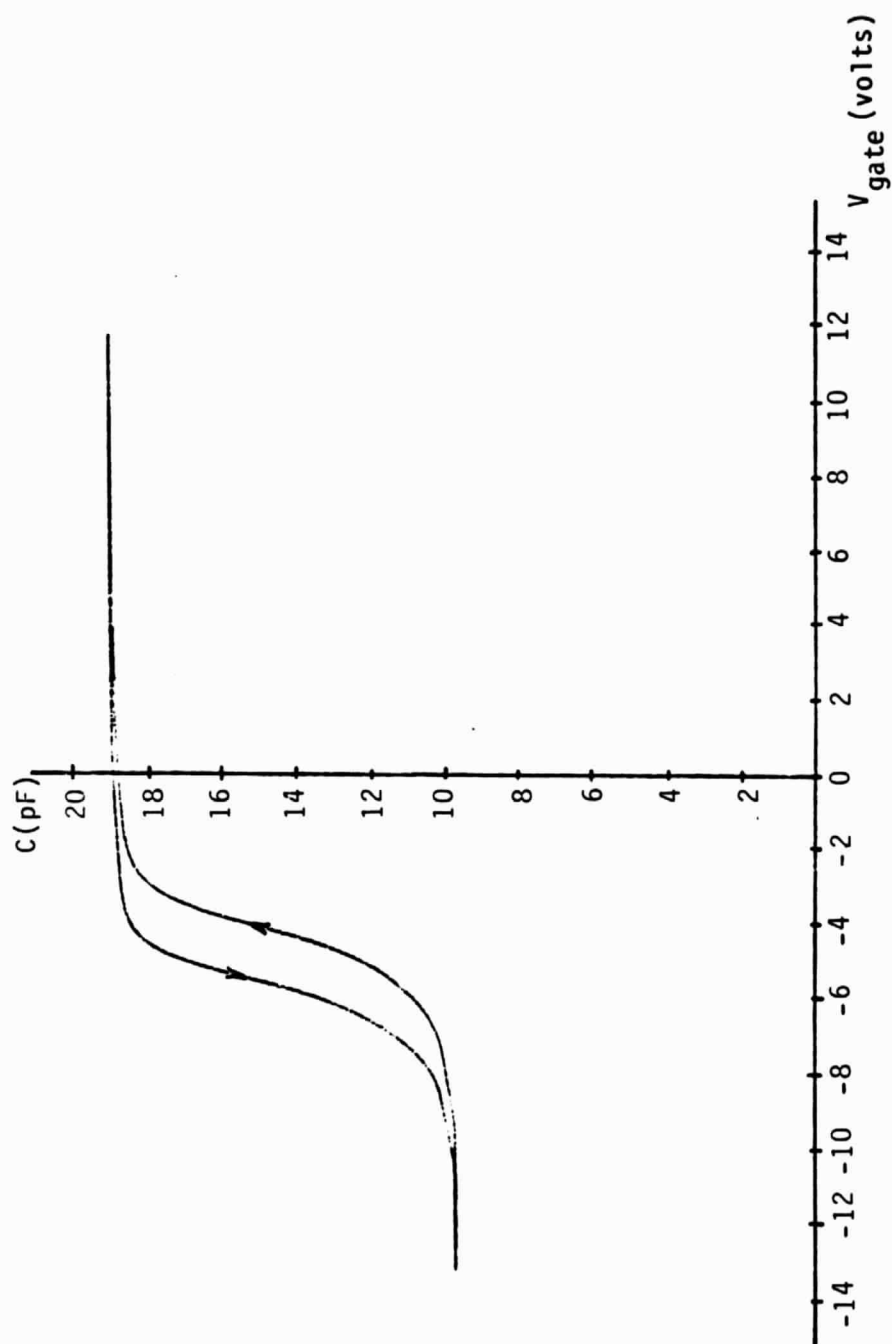


Figure 7. Capacitance-voltage characteristic of an Al-Al<sub>2</sub>O<sub>3</sub>-nSi diode measured at 1 MHz with a gate voltage rate of 0.4 V/sec.

## REFERENCES

1. S. B. Phatak, S. M. Bedair and S. Fugita, Solid State Electron, 23, 839 (1980).
2. N. Chand, P. A. Houston and P. N. Robson, Electronics Lett. 17, 726 (1981).
3. S. Kondo, T. Amano, and H. Nagai, "High Purity LPE Growth of InGaAs by Adding Al to Melt", J. Crystal Growth, 64, (1983) 433-440.
4. K. Bhattacharya and M. Rao, "Growth and Photoluminescence Spectra of High-Purity Liquid Phase Epitaxial  $\text{In}_{.53}\text{Ga}_{.47}\text{As}$ ", J. Appl. Phys. 54, No. 9 (1983) 5096.
5. N. Hakajima, S. Yamazaki, T. Takanohashi, K. Akita, "Liquid Phase Epitaxial Growth of High Purity InGaAs and InP on (100) and (111) B. Faces", J. Crystal Growth, 59 (1982) 572-582.
6. J. D. Oliver, Jr., and L. F. Eastman, "Liquid Phase Epitaxial Growth and Characterization of High Purity Lattice Matched  $\text{Ga}_{1-x}\text{In}_x\text{As}$  on (111) B InP", J. Elect. Materials, 1 (1980) 693.
7. A. J. SpringThorpe, M. Quillec and M. A. Pollack, Appl. Phys. Lett. 35 (1979) 342.
8. S. Iyer, E. K. Stefanakos, A. Abul-Fadl, and W. J. Collis, ACCG-6/ICVEG-6 Conference, New Jersey, July 15-20, 1984 (to be published in J. Crystal Growth).
9. T. Bryskiewicz, J. Lagowski and H. C. Gatos, ACCG-6/ ICVEG-6 Conference, New Jersey, July 15-20, 1984.